Electron affinity of Li: A state-selective measurement

Gunnar Haeffler, Dag Hanstorp, Igor Kiyan,* Andreas E. Klinkmüller, and Ulric Ljungblad
Department of Physics, Göteborg University and Chalmers University of Technology, S-412 96 Göteborg, Sweden

David J. Pegg
Department of Physics, University of Tennessee, Knoxville, Tennessee 37996
(Received 6 November 1995)

We have investigated the threshold of photodetachment of Li^- leading to the formation of the residual Li atom in the $2p^2P$ state. The excited residual atom was selectively photoionized via an intermediate Rydberg state and the resulting Li^+ ion was detected. A collinear laser-ion beam geometry enabled both high resolution and sensitivity to be attained. We have demonstrated the potential of this state-selective photodetachment spectroscopic method by improving the accuracy of Li electron affinity measurements an order of magnitude. From a fit to the Wigner law in the threshold region, we obtained a Li electron affinity of 0.618 049(20) eV. [S1050-2947(96)09105-6]

PACS number(s): 32.80.Fb, 35.10.Hq

I. INTRODUCTION

The four-electron Li^- ion is interesting because of the significant role played by electron correlation in the binding of the outermost electron in this weakly bound system. The major contribution to the correlation energy arises from the interaction of the two valence electrons. Beyond the three-body H^- system, the Li^- ion is most tractable to theory. In the frozen-core approximation, for example, the Li^- ion becomes an effective three-body system consisting of a pair of highly correlated electrons interacting weakly with an inert core. Such a model lends itself well to semiempirical model potential calculations in which the potential experienced by the valence electrons is obtained via spectral information on the eigenvalue spectrum of the Li atom. Most calculations of the electron affinity of Li to date are of this type, e.g. Moccia and Spizzo [1] or Graham *et al.* [2] (and references therein). Recently, however, accurate measurements of this quantity have stimulated *ab initio* calculations [3,4] of comparable accuracy.

The most direct, and potentially the most accurate, method of measuring electron affinities is to use the laser threshold photodetachment (LTP) method [5]. Here one records, as a function of the wavelength of a tunable laser, the onset of production of either photoelectrons or residual atoms in the vicinity of a detachment threshold.

To date, three LTP measurements of the electron affinity of Li have been reported. The earliest such experiment was a crossed laser and ion beam experiment by Feldmann [6]. He utilized an infrared laser to study the $\mathrm{Li}(2s)+\epsilon p$ photodetachment threshold. An accurate threshold energy for a p-wave detachment was difficult to determine because the cross section rises, according to the Wigner law [7], only slowly from zero. Bae and Peterson [8] used collinear laser and ion beams to investigate the total photodetachment cross section around the $\mathrm{Li}(2p)$ cusp situated at the opening of the $\mathrm{Li}(2p)+\epsilon s$ channel. From a careful analysis of this sharp structure they obtained, as one result, an electron affinity value of about the same accuracy as Feldmann. The measurement of Dellwo *et al.* [9] was a direct investigation of the resolved $\mathrm{Li}(2p)+\epsilon s$ channel threshold using photoelectron spectroscopy. In this experiment, however, Doppler broadening associated with the use of crossed laser and ion beams limited the attainable energy resolution.

The electron affinity of Li determined in the present measurement is an order of magnitude more accurate than previous LTP measurements. We utilized resonance ionization [10,11] combined with a collinear laser-ion beam geometry to measure the threshold of the $\mathrm{Li}(2p)+\epsilon s$ partial photodetachment cross section. The state selectivity of the resonance ionization method leads to an excellent signal-to-background ratio. This in turn enabled us to attain a resolution limited only by the laser bandwidth of about 0.2 cm^{-1}. The present threshold energy measurement clearly demonstrates the potential of the method. The concept of combining collinear laser-ion beam spectroscopy with resonance ionization detection was first proposed by Kudryavtsev and Letokohv [12] and later applied to isotope detection measurements by the same authors [13]. Balling *et al.* [14] and Petrunin *et al.* [15] have recently used the same technique in photodetachment measurements.

II. EXPERIMENT

A. Procedure

The two-color state-selective photodetachment experiment described in the present paper is simple in concept. One laser of frequency ω_1 is used to photodetach Li^- ions producing an excited Li atom and a free electron (Fig. 1). A second laser of frequency ω_2 resonantly photoexcites Li atoms left in the $2p$ state to a Rydberg state, which subsequently is field ionized. Hence, the entire process can be represented by the following steps:

*Permanent address: Russian Academy of Science, General Physics Institute, Vavilova St. 38, 117 942 Moscow, Russia.

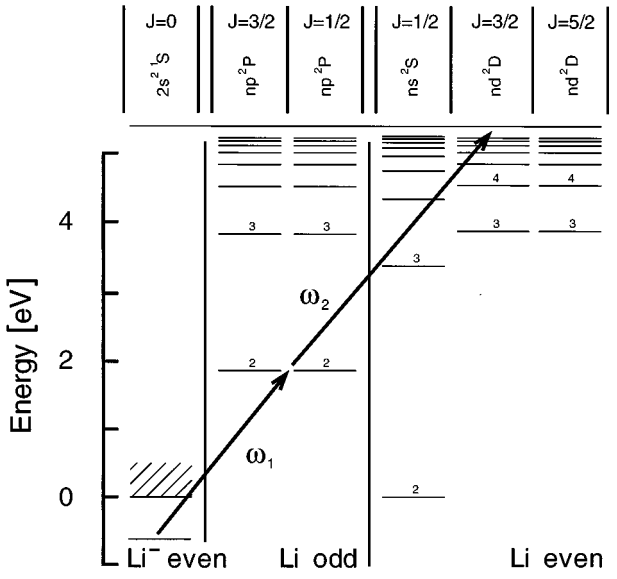

FIG. 1. Excitation scheme: Selected bound states of Li/Li^- grouped according to their parity and total angular momentum. The arrows indicate transitions induced in this experiment.

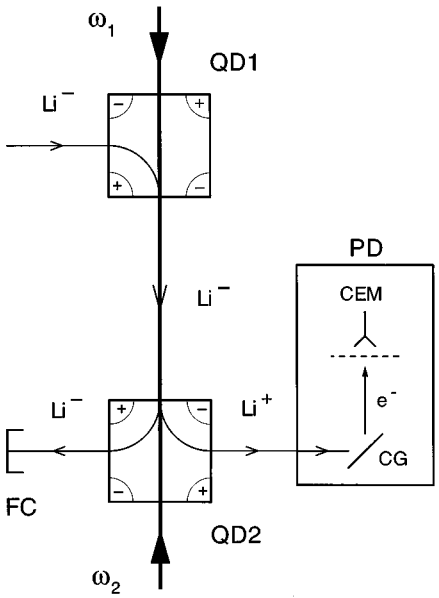

FIG. 2. Interaction-detection chamber: QD1,QD2, electrostatic quadrupole deflectors; CEM, channel electron multiplier; PD, positive-ion detector; FC, Faraday cup; CG, conducting glass plate. Ion and laser beams were merged in the interaction region between the quadrupole deflectors over a common path of 0.5 m.

$$\mathrm{Li}^-(2s^2{}^1S_0)+\hbar\omega_1 \rightarrow \mathrm{Li}(2p^2P_{1/2,3/2})+\mathrm{e}^-,$$

$$\mathrm{Li}(2p^2P_{1/2,3/2})+\hbar\omega_2 \rightarrow \mathrm{Li}(ns,nd),$$

$$\mathrm{Li}(ns,nd) \rightsquigarrow \mathrm{Li}^+(1s^2{}^1S_0)+\mathrm{e}^-, \qquad (1)$$

where $\rightsquigarrow$ denotes field ionization and Li(ns,nd) corresponds to a highly excited Rydberg atom in either a ns or nd state. State selectivity is accomplished in the resonant ionization step since only Li($2p$) atoms can be ionized via the intermediate Rydberg state. In this manner we were able to isolate a particular photodetachment channel, in this case the Li($2p$) channel, and investigate the partial photodetachment cross section by measuring the yield of Li^+ ions.

B. Setup

The $^7Li^-$ ion beam was produced by charge exchange in a cesium vapor cell of a mass selected Li^+ beam from a plasma ion source. An ion current of typically a few nA was obtained in the interaction region. The beam energy was approximately 4 keV.

In the interaction chamber (Fig. 2) the negative ions interacted with laser light in a region defined by two apertures with a diameter of 3 mm placed 0.5 m apart. The ions were deflected in and out of the laser beam by means of two electrostatic quadrupole deflectors whose symmetry axes were perpendicular to the laser and ion beams. The ion current in the interaction region was monitored with a Faraday cup placed after the second quadrupole deflector.

Rydberg atoms formed in the interaction region travel to the second quadrupole where they are ionized by the same electric field that deflects the negative ion beam into the Faraday cup. Positive ions formed in this process were deflected in the opposite direction into a positive-ion detector. In this detector the fast positive ions impinged on a conducting glass plate producing secondary electrons that were detected with a channel electron multiplier (CEM). A metal grid connected to a voltage supply was placed between the glass plate and the CEM. This made it possible to either allow or prevent the secondary electrons from reaching the CEM. The detection efficiency of the positive ion detector was close to unity.

Light of frequency ω_1 was generated by a dye laser operated with Coumarine 307 and light of frequency ω_2 was produced by a dye laser operated with BMQ [2,2‴-dimethyl-*p*-quaterphenyl (see Lamdachrome No. 3570)]. Both dye lasers were pumped by a common XeCl excimer laser. The pulse duration of both lasers was about 15 ns. The maximum energy in a laser pulse delivered into the interaction region was 1.5 mJ for the radiation of frequency ω_1 and 200 μJ for the radiation of frequency ω_2. During the experiment both lasers were attenuated, as will be discussed below.

The two laser pulses counterpropagated in the interaction region and arrived simultaneously in the interaction region. A shift of a few ns between the pulses, occurring at both ends of the interaction region, is negligible since the Li ($2p^2P$) radiative lifetime is 26.99(16) ns [16].

The frequency ω_1 was determined by combining Fabry-Pérot fringes with optogalvanic spectroscopy. The Fabry-Pérot fringes served as frequency markers, whereas transitions of Ne or Ar in a hollow cathode lamp provided an absolute calibration of the energy scale.

III. RESULTS AND DISCUSSION

A. Resonance ionization spectroscopy

First we had to find an appropriate resonance transition for the laser of frequency ω_2. A scan of ω_2, during which ω_1 is set to a frequency far above the Li($2p$) threshold, is shown in Fig. 3. Below the ionization limit we found a wealth of lines. Due to strong saturation, the intensities of

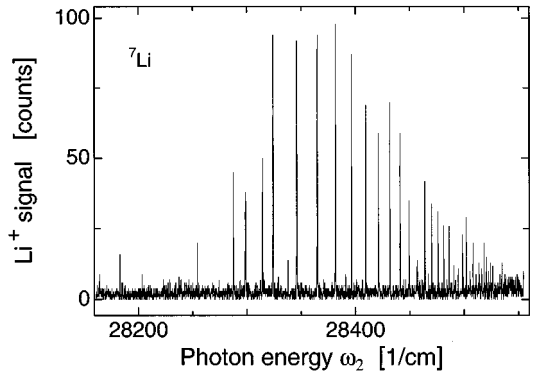

FIG. 3. Rydberg series: Survey of the Rydberg states below the ionization limit of the Li atom. Note how the series terminated at 28 270 cm^{-1}. The lines below that limit we interpret as being due to photoionization. The energy scale is Doppler shifted by -31 cm^{-1}.

the lines are not proportional to the corresponding transition probabilities; close to the ionization limit the detection system became overloaded such that it only recorded one count per laser shot, thus attenuating the strongest lines. For most of the lines we also expect the transition itself to be saturated. The Rydberg series in Fig. 3 exhibits a cutoff at 28 270 cm^{-1}, indicating that the Rydberg atoms were mainly field ionized in an electric field of about 200 kV/m in the second quadrupole deflector. We interpret the lines below the cutoff as being due to photoionization.

A detailed scan of the transition used for the photodetachment threshold measurements is shown in Fig. 4. We identified the two lines as corresponding to transitions from the two fine-structure levels $2p^2P_{1/2,3/2}$ to the same Rydberg state. The measured separation of 0.33(4) cm^{-1} between the two lines in Fig.4 corresponds very well to the fine-structure splitting of 0.337 cm^{-1} of the $2p^2P$ term [17]. The resolved fine structure shown in Fig. 4 demonstrates that the energy resolution of the present collinear beam apparatus is approximately 0.2 cm^{-1}, which is of the same order as the laser bandwidth.

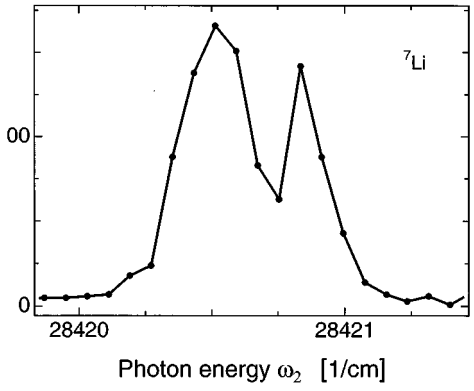

FIG. 4. Fine structure: This spectrum of the fine structure of the $2p^2P$ term is a magnification of the spectrum depicted in Fig. 3. The left peak is due to the transition from the $J=3/2$ level and the right one is due to the transition from the $J=1/2$ level. For the threshold measurements, ω_2 was tuned to the peak of the $J=1/2$ component.The energy scale is Doppler shifted by -31 cm^{-1} .

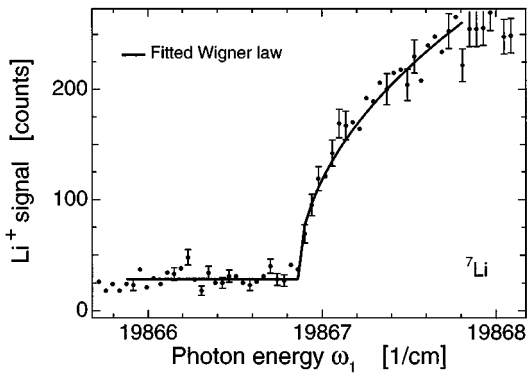

FIG. 5. Li$(2p)+\epsilon s$ threshold: Measurement of the partial relative photodetachment cross section of Li$^-$ around the Li$(2p)$ threshold with antiparallel laser (of frequency ω_1) and ion beam. The solid line is a fit of the Wigner law to the data in the range of the line. The error bars on selected data points represent the shot noise. Notice the very steep onset of the photodetachment and the low background below the threshold. Each data point is obtained from 100 laser pulses.

B. Electron affinity measurements

A typical measurement of the Li$(2p)$ photodetachment threshold with antiparallel laser and ion beams is shown in Fig. 5. The laser frequency ω_2 was held constant and the intensity was set to saturate the transition to the Rydberg state. The frequency ω_1 was then scanned over the Li$(2p)$ threshold.

It was established that two processes contributed to the background, namely, (a)

$$\mathrm{Li}^-(2s^2{}^1S)+\hbar\omega_2 \rightarrow \mathrm{Li}(2p^2P)+\mathrm{e}^-,$$

$$\mathrm{Li}(2p^2P)+\hbar\omega_2 \rightarrow \mathrm{Li}(ns,nd),$$

$$\mathrm{Li}(ns,nd) \rightsquigarrow \mathrm{Li}^+(1s^2{}^1S)+\mathrm{e}^-,$$

and (b) two-electron collisional ionization. Process (a) produced nearly 80% of the background, even though the intensity of the laser light with frequency ω_2 was attenuated. Process (b), two-electron collisional ionization, contributed the remaining background at the operating pressure of 5×10^{-9} mbar (5×10^{-7} Pa). This contribution was found to be proportional to the pressure and is thus dominated by single collision double detachment, as has been discussed previously by Bae and Peterson [18]. The laser intensities were too low for other processes, such as direct two-electron multiphoton detachment, to influence the experiment.

Close to the photodetachment threshold the cross section $\sigma(E)$ is well represented by the Wigner law [7] [Eq. (2)]. If E_0 is the threshold energy and E the photon energy, the Wigner law for electrons detached with different angular momenta l can be written as

$$\sigma(E)\propto(\sqrt{E-E_0})^{2l+1} \quad \text{for } E\geqslant E_0. \tag{2}$$

For the desired first step process in Eq. (1), both s- and d-wave final states for the detached electron are allowed by parity and total-angular-momentum conservation. At the

threshold, however, the s-wave cross section, starting with an infinite slope, completely dominates over the d-wave cross section.

We fitted the Wigner law [Eq. (2)] for s-wave detachment ($l=0$) to the recorded positive ion signal. The data shown in Fig. 5 was recorded with the laser (ω_1) antiparallel to the ion beam. The fit window is the range of the plotted line. The fit yields a value for the red-shifted threshold energy, E_0^r . In order to eliminate the Doppler shift we repeated the measurements using parallel laser and ion beams to determine the blue-shifted threshold energy, E_0^b. The threshold energy corrected for the Doppler to all orders, E_0, is given by the geometric mean of the two measurements:

$$E_0 = \sqrt{E_0^b E_0^r} = 19\,888.55(16)\ \mathrm{cm}^{-1}. \tag{3}$$

The interaction of the induced dipole moment of the atom with the electron will limit the range of validity of the Wigner law. O'Malley [19] obtained an expression that accounts for the residual induced-dipole point-charge interaction,

$$\sigma(k) \propto k^{2l+1}\left[1 + \frac{4\alpha k^2 \ln k}{(2l+3)(2l+1)(2l-1)} + \mathcal{O}(k^2)\right], \tag{4}$$

where $k=\sqrt{2(E-E_0)}$ and α is in atomic units. This equation can be used to estimate an approximate range of validity for the Wigner law by determining the conditions under which the second term, and therefore higher terms, become negligible. With a dipole polarizibility of $\alpha=152$ a.u. for the Li $2p^2P$ state [20], the second term is much less than unity up to 1 cm^{-1} above the threshold, and consequently the Wigner law should be applicable over this range. This, of course, assumes that there are no resonances in this region, a condition that has been previously established by Dellwo *et al.* [9].

Saturation of the signal can originate in the photodetachment process or the detection system. In the data shown in Fig. 5 the detection system starts to saturate at about 250 counts (for 100 laser pulses). We attenuated the intensity of the laser of frequency ω_1 sufficiently to avoid any saturation of the signal within the first 1.0 cm^{-1} above the threshold.

To determine the electron affinity of Li we had to subtract the well known $2p^2P_{1/2} \rightarrow 2s^2S$ transition energy of 14 903.648 130(14) cm^{-1} [17] from the measured Doppler-corrected threshold energy E_0 [Eq. (3)]. We determined the Li electron affinity to be 4 984.90(17) cm^{-1}. There are two major contributions to the error: 0.13 cm^{-1} is due to a calibration uncertainty of the hollow cathode lamps, and the rest is due to statistical scattering of the fitted threshold values.

TABLE I. Comparison of different measurements and calculations of the Li electron affinity.

Author	Affinity in meV
Experiment:	
This work	618.049±0.020
Feldmann (1976) [6]	618.2±0.5
Bae and Peterson (1985) [8]	617.3±0.7
Dellwo *et al.* (1992) [9]	617.6±0.2
Theory (after 1992):	
Chung and Fullbright (1992) [3]	617.4±0.2
Froese Fischer (1993) [4]	617.64

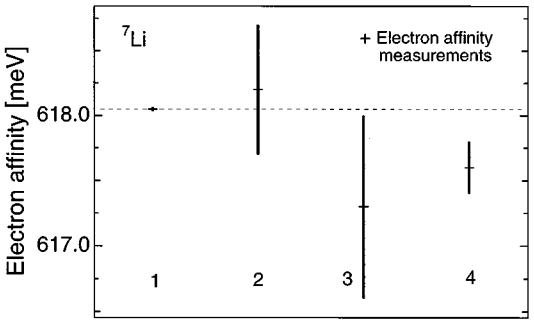

FIG. 6. Electron affinity: Graphical comparison of the different experimental lithium electron affinity values with their respective uncertainties. From left to right the values are as follows: 1, this work; 2, Feldmann; 3, Bae *et al.*; and 4, Dellwo *et al.* For references see Table I.

In order to convert our electron affinity in cm^{-1} to eV we used the recommended factor of (1/8 065.5410) [eV/(cm^{-1})] [21] and obtained 0.618 049(20) eV. In Fig. 6 this value is compared with previous experiments. These values are also compiled in Table I together with some recently calculated Li electron affinities.

IV. SUMMARY AND CONCLUSION

We have demonstrated that photodetachment spectroscopy combined with resonance ionization is a powerful method for studying partial photodetachment cross sections of negative ions. The collinear beam geometry simultaneously provides high sensitivity, due to the large interaction volume, and excellent resolution, due to velocity compression. In addition, removal of the Doppler shift to all orders can be achieved by the use of two separate measurements involving parallel and antiparallel laser and ion beams. Both merits can be fully retained for channel specific photodetachment investigations with the excitation scheme used in this experiment. Our improved Li electron affinity of 0.618 049(20) eV reveals the potential of this method, and this method can, in principle, be extended to essentially all elements. We are currently developing this type of state-selective detection scheme in connection with ongoing studies of high-lying doubly excited states of the Li^- ion [22].

ACKNOWLEDGMENTS

Financial support for this research has been obtained from the Swedish Natural Science Research Council (NFR). Personal support was received from the Wenner-Gren Center Foundation for Igor Kiyan. D. P. acknowledges the support from the Swedish Institute and the U.S. Department of Energy, Office of Basic Energy Sciences, Division of Chemical Sciences.

[1] R. Moccia and P. Spizzo, J. Phys. B **23**, 3557 (1990).
[2] R. L. Graham, D. L. Yeager, and A. Rizzo, J. Comput. Phys. **91**, 5451 (1989).
[3] K. T. Chung and P. Fullbright, Phys. Scr. **45**, 445 (1992).
[4] C. Froese Fischer, J. Phys. B **26**, 855 (1993).
[5] D. M. Neumark, K. R. Lykke, T. Andersen, and W. C. Lineberger, Phys. Rev. A **32**, 1890 (1985).
[6] D. Feldmann, Z. Phys. A **277**, 19 (1976).
[7] E. P. Wigner, Phys. Rev. **73**, 1002 (1948).
[8] Y. K. Bae and J. R. Peterson, Phys. Rev. A **32**, 1917 (1985).
[9] J. Dellwo, Y. Liu, and D. J. Pegg, Phys. Rev. A **45**, 1544 (1992).
[10] G. S. Hurst, M. G. Payne, S. D. Kramer, and J. P. Young, Rev. Mod. Phys. **51**, 767 (1979).
[11] G. S. Hurst and M. G. Payne, *Principles and Applications of Resonance Ionization Spectroscopy* (Techno House, Bristol, England, 1988).
[12] Y. A. Kudryavtsev and V. S. Letokohv, Appl. Phys. B **29**, (1982).
[13] Y. A. Kudryavtsev, V. S. Letokohv, and V. V. Petrunin, Opt. Commun. **68**, 25 (1988).
[14] P. Balling *et al.*, J. Phys. B **26**, 3531 (1993).
[15] V. V. Petrunin *et al.*, Phys. Rev. Lett. **75**, 1911 (1995).
[16] W. I. McAlexander *et al.*, Phys. Rev. A **51**, R871 (1995).
[17] C. J. Sansonetti and B. Richou, Bull. Am. Phys. Soc. **40**, 1272 (1995).
[18] Y. K. Bae and J. R. Peterson, Phys. Rev. A **37**, 3254 (1988).
[19] T. F. O'Malley, Phys. Rev. **137**, A1668 (1965).
[20] N. L. Manakov, V. D. Ovsyannikov, and L. P. Rapoport, Opt. Spectrosc. **38**, 115 (1975).
[21] E. R. Cohen and B. N. Taylor, J. Phys. Chem. Ref. Data **17**, 1795 (1988).
[22] U. Berzinsh *et al.*, Phys. Rev. Lett. **74**, 4795 (1995).